Available online at www.sciencedirect.com
SCIENCE DIRECT®
Biochemical and Biophysical Research Communications 332 (2005) 157–166
BBRC
www.elsevier.com/locate/ybbrc

An N-terminal nuclear localization sequence but not the calmodulin-binding domain mediates nuclear localization of nucleomorphin, a protein that regulates nuclear number in *Dictyostelium*

Michael A. Myre [1], Danton H. O'Day *

Department of Biology, University of Toronto at Mississauga, Mississauga, Ont., Canada

Received 11 April 2005
Available online 27 April 2005

Abstract

Nucleomorphin is a novel nuclear calmodulin (CaM)-binding protein (CaMBP) containing an extensive DEED (glu/asp repeat) domain that regulates nuclear number. GFP-constructs of the 38 kDa NumA1 isoform localize as intranuclear patches adjacent to the inner nuclear membrane. The translocation of CaMBPs into nuclei has previously been shown by others to be mediated by both classic nuclear localization sequences (NLSs) and CaM-binding domains (CaMBDs). Here we show that NumA1 possesses a CaMBD (^{171}EDVSRFIKGKLLQKQQKIYKDLERF^{195}) containing both calcium-dependent-binding motifs and an IQ-like motif for calcium-independent binding. GFP-constructs containing only NumA1 residues 1–129, lacking the DEED and CaMBDs, still localized as patches at the internal periphery of nuclei thus ruling out a direct role for the CaMBD in nuclear import. These constructs contained the amino acid residues ^{48}KKSYQDPEIIAHSRPRK^{64} that include both a putative bipartite and classical NLS. GFP-bipartite NLS constructs localized uniformly within nuclei but not as patches. As with previous work, removal of the DEED domain resulted in highly multinucleate cells. However as shown here, multinuclearity only occurred when the NLS was present allowing the protein to enter nuclei. Site-directed mutation analysis in which the NLS was changed to ^{48}EF^{49} abolished the stability of the GFP fusion at the protein but not RNA level preventing subcellular analyses. Cells transfected with the ^{48}EF^{49} construct exhibited slowed growth when compared to parental AX3 cells and other GFP-NumA1 deletion mutants. In addition to identifying an NLS that is sufficient for nuclear translocation of nucleomorphin and ruling out CaM-binding in this event, this work shows that the nuclear localization of NumA1 is crucial to its ability to regulate nuclear number in *Dictyostelium*.

Keywords: Calmodulin-binding domain; IQ motif; Nuclear localization sequence; *Dictyostelium*; Nuclear number; Growth

Nucleomorphin (NumA) is the first nuclear calmodulin-binding protein (CaMBP) to be identified in *Dictyostelium discoideum* where it was shown to be involved in regulating nuclear number [1]. Nucleomorphin exists as two predominant isoforms NumA1 and NumA2 (formerly NumA and B) that show different patterns of expression during growth, starvation, and development [2]. The C-terminal sequence of the larger isoform, NumA2, is identical to that of the N-terminus of NumA1. However, this isoform differs from NumA1 in that it contains a single N-terminal breast cancer carboxy-terminus (BRCT) domain. The originally identified NumA1 cDNA encodes a novel, 43 kDa acidic protein possessing an extensive glutamic/aspartic acid region (DEED) that binds to the calcium-binding protein CBP4a [1,2]. Previous work verified NumA1 as a

* Corresponding author. Fax: +1 905 828 3792.
E-mail address: doday@utm.utoronto.ca (D.H. O'Day).
[1] Present address: MassGeneral Institute for Neurodegenerative Disease, Harvard Medical School, Massachusetts General Hospital, 114 16th Street, USA.

0006-291X/$ - see front matter © 2005 Elsevier Inc. All rights reserved.
doi:10.1016/j.bbrc.2005.04.101

CaMBP but its binding domain remained to be characterized. Although there are no NumA1 homologs in any of the searchable databases, the DEED domain shares similarity to the conserved nucleoplasmin domain of the nucleoplasmin superfamily of nuclear proteins that are involved in chromatin remodeling and to the yeast Mak16 protein that also has been implicated in cell cycle progression [3–5]. Expression of GFP-fusion dominant-negative mutants lacking the DEED region results in highly multinucleate cells [1]. In total, a potential nuclear role for nucleomorphin in cell cycle regulation has been proposed [6]. However, nothing is known about the way NumA1 is localized to the nucleus, the importance of this localization or if the localization affects cell function.

Many studies have shown that most nuclear proteins are imported into the nucleus in a signal-dependent manner [7]. In general, the typical nuclear localization sequence (NLS), as exhibited by the SV40 large T antigen (PKKKRKV), comprises seven residues characterized by a high content of basic amino acids. Variations on this NLS include the bipartite-type originally identified in nucleoplasmin (KR-10aa-KKKL) that consists of two clusters of basic amino acids separated by 10 amino acids [8]. While a number of studies have been carried out on the nuclear localization and function of CaM, comparatively few have focused on the role of CaM in nuclear translocation. The results of these studies show that, depending on the protein, CaM may have indirect, direct or no effect on protein translocation into the nucleus. Various CaM antagonists (e.g., calmidazolium, W7, and W12) block the GTP-independent nuclear import of the SV40 large T antigen NLS in HeLa cells [9]. Calmodulin was shown to be directly involved in the translocation of the transcription factor SOX9 (Sry-related HMG box 9) into the nucleus of Sertoli cells during mammalian sex determination since this translocation requires the presence of the SOX9 CaMBD [10]. The nuclear import of c-Rel and RelA, both Ca^{2+}-dependent CaM-binding members of the NFκB/Rel family, is differentially regulated [11]. CaM-binding deficient mutants of c-Rel but not of RelA lead to increased nuclear import and resultant transcriptional activity revealing that CaM specifically inhibits the nuclear import of c-Rel [11]. In contrast, while CaMKIV possesses a CaM-binding domain and a putative NLS localized within the C-terminus of this protein neither of these mediates import of this kinase into the nucleus of HEK293A cells, instead the protein kinase homology domain alone oversees nuclear import [12]. Several nuclear proteins of *Dictyostelium*, including Dd-STAT proteins, skp1 and Hsp32, have been identified and functionally characterized but an experimentally determined NLS has not been determined for any of these proteins and the role of CaM in nuclear localization has not been addressed [13–15].

Because of the potential significance of nucleomorphin as a cell cycle protein and evidence for its role in regulating nuclear number, we set out to further characterize the CaM-binding domain and its relationship to nuclear import. Since the active import of a protein into the nucleus typically requires the presence of an NLS in the sequence of the imported protein, we further investigated the sequence-dependent nuclear translocation of nucleomorphin using GFP-NumA1 deletion mutants. We show here that the N-terminal amino acid residues containing the sequence ^{48}KKSYQDPEIIAHSRPRK^{64} are critical for nuclear localization. When fused to GFP these residues alone were able to increase its nuclear distribution. In contrast, the absence of the CaMBD had no effect on nuclear localization, indicating that this domain is not directly involved in nuclear translocation. Our data indicate that the nuclear localization of NumA1 is central to its ability to regulate nuclear number in *D. discoideum*.

Materials and methods

All restriction enzymes used were purchased from Amersham Pharmacia. T4 DNA ligase was from New England Bio Labs. All media reagents were from BioShop Canada and VWR Scientific Products. Low DNA mass ladders were from Gibco-BRL. PCR molecular weight markers and the mini-complete protease inhibitor cocktail tablet were from Boehringer–Mannheim. Western blots were analyzed using the Molecular Dynamics Storm gel and blot system. T7·Tag antibody agarose was purchased from Novagen. One-step RT-PCR, PCR primers, and the Qiaex II Gel Extraction system were from Qiagen. Monoclonal mouse anti-GFP antibody was purchased from Sigma. All constructs were sequenced from the 5′-end to ensure the GFP-fusion protein was in-frame at the Hospital for Sick Children, Toronto, Ont., Canada. The pTX-GFP vector was a gift from Dr. Thomas Egelhoff.

Cell culture. Vegetative cells of *D. discoideum* AX3 were grown axenically in HL-5 at 22 °C as described elsewhere [1]. Transformed cells expressing the GFP-NumA1 fusion constructs were grown axenically in shaking cultures supplemented with 10 μg/mL G418. The average cell density was determined by taking an aliquot of culture and counting it in a hemocytometer.

CaM-binding constructs: construction and expression of pET-21b (+) vectors. The nucleomorphin-encoded genes were amplified using the PCR from the originally isolated λZAP cDNA expression library clone [1]. Primers were designed for deletion analysis of the NumA1 CaM-binding domain (Table 1). Eight deletion constructs were designed and tested for their CaM-binding ability. Construction and expression of NumAΔ118–167, lacking the DEED repeat, is detailed elsewhere [1]. The amplified NumA1 cDNA sequences were digested using the restriction enzymes *Sac*I and *Xho*I, and then ligated into the vector pET-21b (+) (Novagen) as per the manufacturer's recommendations. Plasmids were screened for an insert using the restriction enzymes *Sac*I and *Xho*I, sequenced, and designated NumAΔN45$^{(\Delta 118–167)}$, NumAΔN98$^{(\Delta 118–167)}$, NumAΔN216, NumAΔC26$^{(\Delta 118–167)}$, NumAΔC76$^{(\Delta 118–167)}$, NumAΔC97$^{(\Delta 118–167)}$, and NumAΔC211, respectively. ΔN and ΔC indicate N- and C-terminal mutants, and the numbers specify the number of amino acids deleted from the respective end. Recombinant protein expression was induced with the addition of 0.6 mM isopropyl-thio-β-galactopyranoside to the media. Cells were harvested and then lysed by sonication in 10 mM

Table 1
Primer used in CaM-binding deletion analysis

Length (bp)	Primer pair 5′–3′	Protein
904	aaagagctcatggatgttcatttaacatcatcgacatc aaactcgagttaatttgagggtaaagacataaaaaatgcact	NumAΔ118–167
760	aaatttaaagagctcatatcaagatccagag aaactcgagttaatttgagggtaaagacataaaaaatgcact	NumAΔN45
601	tctaaataggagctcaactacatcaggaggc aaactcgagttaatttgagggtaaagacataaaaaatgcact	NumAΔN98
385	aagatctaggagctcatctagagattatatcg aaactcgagttaatttgagggtaaagacataaaaaatgcact	NumAΔN216
826	aaagagctcatggatgttcatttaacatcatcgacatc ctaatgtcgctcgagttagtaagaatggttttttg	NumAΔC26
676	aaagagctcatggatgttcatttaacatcatcgacatc taaacaagtctcgagttatggtattattacctccatcttgg	NumAΔC76
613	aaagagctcatggatgttcatttaacatcatcgacatc tcttctttgctcgagttaaaggtatttgtttctcac	NumAΔC97
403	aaagagctcatggatgttcatttaacatcatcgacatc atcttcttcctcgagcacttaatcatcatatttatac	NumAΔC211

Incorporated restriction sites for *Sac*I and *Xho*I are underlined.

Tris, pH 7.0, supplemented with a mini-complete protease inhibitor cocktail buffer.

NLS analysis: PCR-mediated site-directed mutagenesis of NumA1. Construction of the pGFP-NumA1 vector has been previously described [1]. All primers used for the deletion analysis of NumA1 are listed in Table 2.

PGFP NumAΔ48–64EF. We used the PCR to create an in-frame deletion of residues 48–64 within NumA1. The resultant mutation replaces these 18 residues with an *Eco*RI site, which codes for both glutamic acid (E) and phenylalanine (F), respectively. This strategy uses the same forward primer for the GFP-NumA1 construct, and a mutagenic reverse primer designated mutN, with a restriction site for *Eco*RI. The NumAmutN PCR product was agarose gel purified and digested with the restriction enzymes *Sac*I and *Eco*RI, ligated into pUC19 pre-cut with *Sac*I and *Eco*RI, and named pUCNumAmutN. Digests with *Eco*RI and *Pst*I liberate the NumAmutN′ fragment that was then agarose gel purified. Using the same reverse primer for the GFP-NumA1 construct and a mutagenic forward primer designated mutC, also with a restriction site for *Eco*RI, we used the PCR to amplify NumAmutC. The NumAmutC PCR product was agarose gel purified, digested with the restriction enzymes *Xho*I and *Eco*RI, ligated into pDRIVE pre-cut with *Xho*I and *Eco*RI, and named pDNumAmutC. The purified NumAmutN′ fragment was then ligated into pDNumAmutC pre-cut with *Eco*RI and *Pst*I, and named pDNumAΔNLS. Digests with *Sac*I and *Xho*I liberate the NLS mutagenized NumA1 fragment where it was agarose gel purified, ligated into pTXGFP pre-cut with *Sac*I and *Xho*I, transformed by electroporation into *Escherichia coli* DH5α, purified, sequenced, and named pGFP-NumAΔ48–64EF. ΔN and ΔC indicate N- and C-terminal mutants, and the numbers specify the number of amino acids deleted from the respective end.

Table 2
Primers used in NLS deletion analysis

Length (bp)	Primer pair	Amino acids
1042	aaagagctcatggatgttcatttaacatcatcgacatc aaactcgagttaatttgagggtaaagacataaaaaatgcact	1–340
198	aaagagctcatggatgttcatttaacatcatcgacatc cttgataactgaattctaaatttaaaagatgattctttttttgtgag	1–46
825	ccaagaaaagaattcggtggtgtttctttggtagaggcactatc aaactcgagttaatttgagggtaaagacataaaaaatgcact	68–340
403	aaagagctcatggatgttcatttaacatcatcgacatc atcttcttcggatccacttatcatcatatttatac	1–129
552	gaaagtgatgagctcgattttgatagtgatga aaactcgagttaatttgagggtaaagacataaaaaatgcact	161–340

pGFP NumAΔC211. Primers were designed to amplify the region encoding amino acids 1–129 of NumA1. *Sac*I and *Xho*I restriction sites were added to the 5′- and 3′-ends, respectively, using the primers pNumAF and pNumNRev.

pGFP NumAΔN160. Primers were designed to amplify the region encoding amino acids 161–340. *Sac*I and *Xho*I restriction sites were added to the 5′- and 3′-ends, respectively, using the primers pNumAR and pNumCtRev.

pGFP-^{48}NLS^{64}. Primers were designed to amplify the region encoding amino acids 48–64. *Sac*I and *Xho*I restriction sites were added to the 5′- and 3′-ends, respectively, using the primers pNLS-GFP-F and pNLS-GFP-R. Plasmid was purified, sequenced, and named pGFP-^{48}NLS^{64}.

Transformation of Dictyostelium with pGFP-NumA1, pGFP-NLS, pGFP NumAΔC211, pGFP NumAΔN160, pGFP NumAΔ118–167, and pGFP NumAΔ142–198. Cells were transformed by electroporation in triplicate essentially as described elsewhere, and deposited into three separate six-well culture plates [16]. Colonies could be observed by the third day of antibiotic selection. Single colonies were aspirated using sterile Pasteur pipettes into 2 mL HL-5 containing 10 μg/mL G418 and grown axenically to saturation as described above.

SDS–PAGE and Western blotting analysis of NumA1 deletion mutants. Total cell protein samples were quantified using the BioRad protein dye assay. Protein samples equal to 20 μg were loaded onto 15% polyacrylamide gels. The protein was resolved by gel electrophoresis at 140 V for ~2 h. Gels were stained with Coomassie blue and then destained overnight in destain solution (40% MeOH, 10% glacial acetic acid) or protein transferred to PVDF membrane, probed with either monoclonal anti-GFP (mouse IgG1 isotype) (1:2000) (Sigma) or polyclonal antibodies raised to NumAΔC211 (1:100). Secondary anti-mouse or anti-rabbit HRP-conjugated antibodies (DAKO) were used at a 1:100 dilution and detected with ECL Plus using the Molecular Dynamics Storm gel and blot system.

Reverse transcription-polymerase chain reaction analysis. AX3 cells and cells transformed with GFP-NumA1 deletion constructs were grown in shaking cultures as described above. Using TRIzol, total RNA was purified from the respective experimental cultures after which reverse transcription-polymerase chain reaction (RT-PCR) was performed for 30 cycles as per the manufacturer's recommendations with primers specific for NumA1 and GFP. Negative controls were performed in which the reverse transcriptase amplification step was omitted.

Fluorescence microscopy. To record the distribution of GFP-NumA1 fusion constructs in living cells, cells were grown to a density of 3×10^6 cells/mL, washed in low ionic strength DB buffer, resuspended at a density of 1×10^7 cells/mL, and applied to coverslips as described [1]. To observe nuclei, cells were stained with Hoechst 33258. Cells were viewed using a Zeiss-Axioskop epifluorescence microscope with a 100× Zeiss Plan-Neofluar oil immersion objective. Images were captured using a mounted mono-10 Bit Q1CAM camera as digital files using Northern Eclipse V5.5. At least 300 cells from each experiment were examined and the number of nuclei per cell was counted.

Pull-down assay for calmodulin-binding. Fifty microliter calmodulin–agarose beads aliquoted into individual microcentrifuge tubes was washed once in 200 μL of binding buffer (10 mM Tris, pH 8.0, 150 mM NaCl, and 5 mM $CaCl_2$ or 10 mM EGTA or 60 μM W-7), spun, and the supernatant was removed. One milliliter of binding buffer was added and the beads were pre-activated for 1 h with rotation at 4 °C, spun, and the supernatant was removed. One milliliter of fresh binding buffer was added and the reaction mixture was incubated with 10 μg/mL of the target protein for 2 h at 4 °C with rotation. After

centrifugation, the beads were washed three times in wash buffer (20 mM Hepes, pH 7.4, 150 mM NaCl, 5 mM sodium pyrophosphate, 1% glycerol, and 1% Triton X-100, supplemented with 5 mM $CaCl_2$ or 10 mM EGTA), once in wash buffer for 1 h at 4 °C with rotation, and once in 10 mM Hepes, pH 7.4. The samples were boiled in 20 μL of 2× SDS–PAGE sample buffer and analyzed by Western blotting.

Results and discussion

Identification of the CaM-binding region of NumA1

Nucleomorphin is a nuclear calmodulin-binding protein that localizes as patches within the nucleoplasm adjacent to the nuclear membrane [1]. Current models for predicting Ca^{2+}-dependent CaM-binding domains are based on loosely conserved continuous domains consisting of ~20 amino acids that contain critical hydrophobic residues at specific positions [17,18]. Initial analyses of NumA1 using the Calmodulin Target Database identified three putative Ca^{2+}-dependent CaM-binding domains and deletion constructs failed to define the CaM-binding region or to rule out any of those putative domains. Recent sequence analysis of this region using the current version of the binding site search function at the Calmodulin Target Database (http://calcium.uhnres.utoronto.ca/ctdb/ctdb/sequence.html) predicted a single CaM-binding domain spanning 25 residues (171–195) in the carboxy-terminus (Fig. 1A) [19]. To test whether this region of NumA1 was responsible for CaM-binding we generated a series of eight T7-tagged NumA1 deletion constructs that were expressed in *E. coli* (Figs. 1A and B). These constructs were designed to lack the DEED (46 glu/asp in a 52 aa sequence) repeat since this limits NumA1 expression in bacterial hosts presumably due to the excess requirement for glutamic and aspartic acid residues [1]. That study also showed that the DEED repeat was not involved in CaM-binding. As can be seen from the input lanes in Fig. 1, all of the constructs were expressed efficiently in *E. coli*. Bacterial cell lysates containing expressed recombinant NumA1 deletions were incubated with CaM–agarose in the presence of Ca^{2+} or EGTA. NumA1 was retained on CaM-agarose in the presence of both 5 mM Ca^{2+} and 10 mM EGTA (Fig. 1B). The binding to CaM was specific even in the presence of many unrelated bacterial proteins, but could be abolished by the addition of 60 μM W-7 (Fig. 1B). Of the eight deletion constructs tested all were retained on CaM-agarose in the presence of Ca^{2+} and/or EGTA except for NumAΔN216 and NumAΔC211 (Fig. 1B). These two constructs are each missing a region comprised of 48 residues that contains three predicted Ca^{2+}-dependent CaM-binding motifs (1-5-10, 1-5-16, and 1-14) each of which shows an appropriate distribution of hydrophobic residues as shown by helical wheel analysis (Figs. 2A–E). Except for NumAΔN98, which

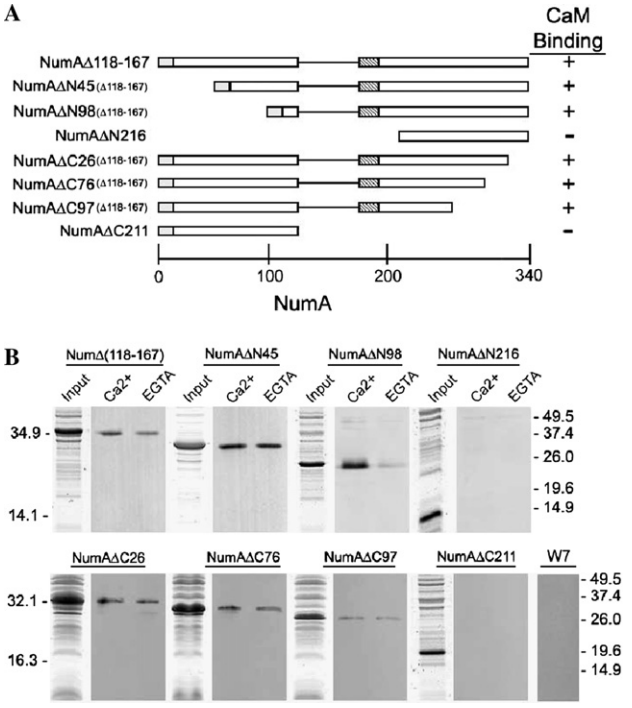

Fig. 1. Ca^{2+}-dependent/independent binding of NumA1 deletion mutants from cellular lysates to CaM–agarose. Cellular lysates from bacterial strain BL21 expressing NumA1 deletion mutants were incubated with CaM–agarose in the presence of Ca^{2+} or EGTA. (A) Localization of the CaM-binding region of NumA1. A schematic representation of each deletion mutant is shown. The names of each construct are listed on the left. CaM-binding is shown on the right (+, binding; −, no binding). (B) BL21 cell cultures were induced with 0.6 mM IPTG for ~3 h, collected by centrifugation, and washed and lysed in an appropriate volume of lysis buffer. Each of the samples was incubated with CaM–agarose beads in the presence of Ca^{2+}, EGTA or 60 μM W-7. Bound CaMBPs were resolved on 15% SDS–PAGE, transferred to PVDF membrane, probed using monoclonal anti-T7-Tag HRP-conjugated antibodies, and detected with ECL Plus using the Molecular Dynamics Storm blot system. MW marker positions (kDa) are given on the right. Input: SDS–PAGE of total protein extract; Ca^{2+} (5 mM); EGTA (10 mM).

showed decreased binding in the presence of EGTA, the amount of each construct that was retained on CaM–agarose was relatively the same in the presence of either Ca^{2+} or EGTA. The decreased binding of NumAΔN98 in the presence of EGTA may have been a result of improper folding when expressed in a bacterial host under the conditions we used. Based on previous work the Ca^{2+}-independent binding of NumA1 was unexpected. Ca^{2+}-independent binding is often mediated by IQ or IQ-like motifs [20]. In keeping with this the identified CaM-binding region was found to contain an IQ-like motif that shares similarities to other such motifs (Fig. 2D). Thus, the region required for CaM-binding to NumA1 appears to be ~25 amino acids in length containing both an IQ motif and three overlapping 1-5-10, 1-16, and 1-4 motifs which could mediate Ca^{2+}-independent and Ca^{2+}-dependent binding, respectively (Fig. 2A).

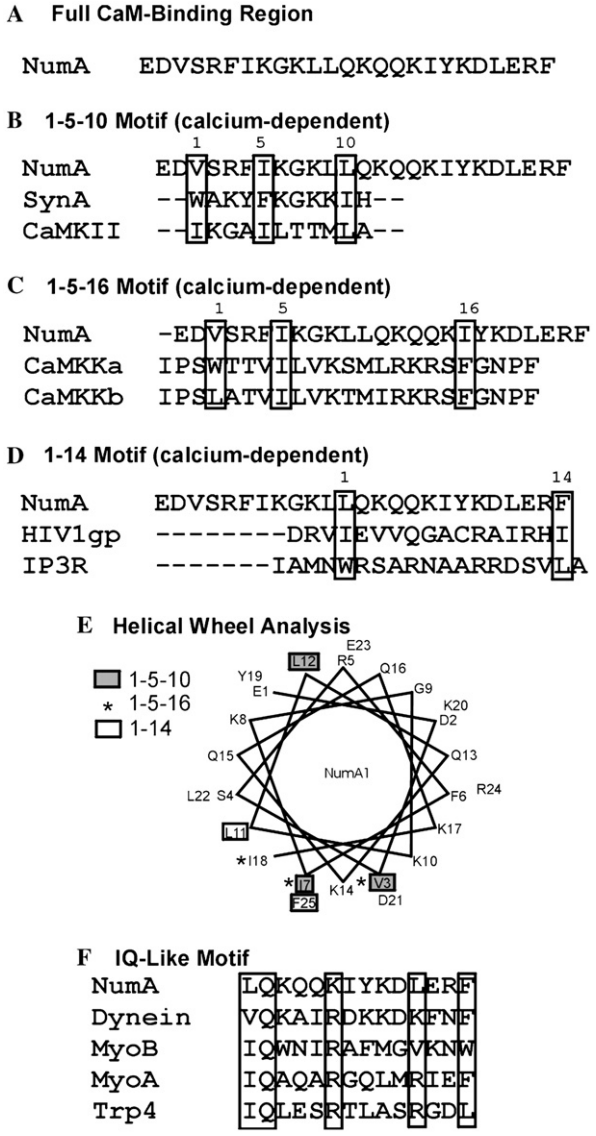

Fig. 2. The CaM-binding domains of nucleomorphin. (A) The full CaM-binding region of NumA1 identified using the Calmodulin Target Database (http://calcium.uhnres.utoronto.ca). (B–D) Clustal alignment of selected Ca^{2+}-dependent 1-5-10 (B), 1-5-16 (C), and 1-14 motifs [17,18,30]. (E) Helical wheel analysis showing positions of hydrophobic amino acids of the putative Ca^{2+}-dependent CaM-binding motifs. The 1-5-10 and 1-516 motifs share initial hydrophobic residues. (F) Ca^{2+}-independent IQ-like motifs (C) aligned with NumA1. Each protein sequence is aligned according to the consensus motif. The locations of conserved hydrophobic residues that are thought to play an important role in the interaction with CaM are shown (boxed). SynA, synapsin 1A, CaMKII, rat CaM-dependent kinase II; CaMKKa,b, CaM-dependent kinase kinases α and β; HIV1gp, HIV glycoprotein 160; IP3R, rat IP3 receptor; MyoB, human cardiac myosin β; MyoA, human cardiac myosin α; Tryp4, bovine Tryp4.

The N-terminal region but not the CaM-binding domain is needed for nuclear localization

GFP-NumA1 localizes specifically within the nucleoplasm as distinct patches adjacent to the inner nuclear membrane [1]. The NLSs determined experimentally in many nuclear proteins typically contain clusters of basic amino acids that may occur as a single entity or in concert as multiple signal sequences, and typically conform to the classical (T-ag—^{126}PKKKRKV^{132}) or bipartite-type (nucleoplasmin—^{156}KR-10 aa-KKKL^{171}) [7,16,21]. Since *Dictyostelium discoideum* evolved early during the plant/fungi/animal split, it possesses many phylogenetic attributes common to each group. For example, while *Dictyostelium* phosphoglycerate kinase and thymidine kinase are most similar to mammalian proteins, *Dictyostelium* histone H1 is fundamentally plant-like [2,22–24]. For this reason, sequence analysis of NumA1

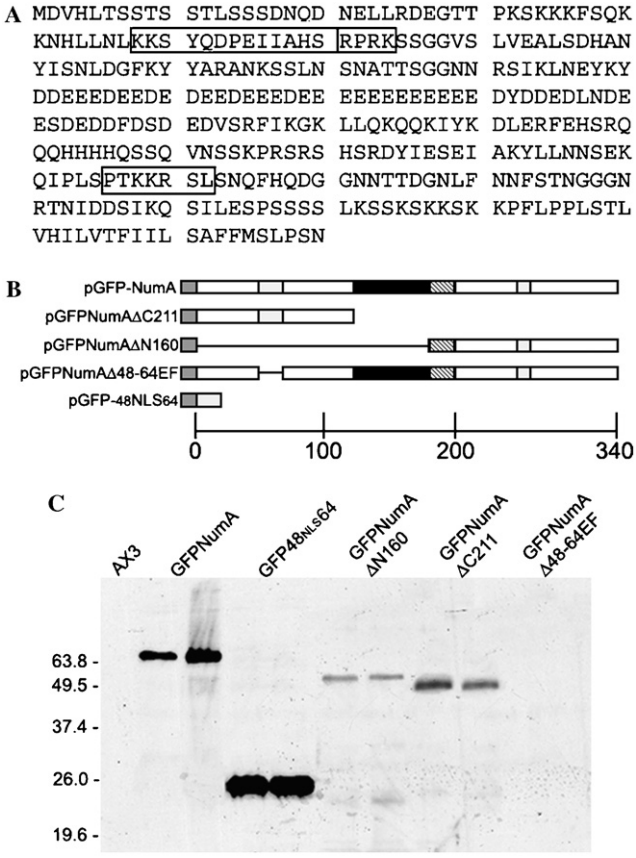

Fig. 3. Deletion analysis of the NumA1 NLS. (A) Four predicted NLS domains are boxed within the NumA1 amino acid sequence. (B) A schematic representation of green fluorescent protein (GFP)-NumA1 deletion constructs. Each NumA1 sequence is attached to the C-terminus of the GFP sequence (dark gray). Other domains include the DEED domain (shaded black); predicted NLS (gray); CaM-binding domain (striped). Scale bar depicts the length in amino acids. (C) Western analysis of GFP-NumA1 deletion mutants. Cultures of *D. discoideum* AX3 cells were transfected with the GFP-NumA1 deletion constructs. Cell lysates were analyzed by monoclonal anti-GFP antibody. Results are of two representative clones from six independent transformations. Signals detected were of the predicted sizes except no signal was detected for GFPNumAΔ48–64EF mutant transformants. Lane 1 AX3 represents the *negative* control of cells not transformed with a GFP-construct. Molecular weight size markers are indicated on the left in kilodaltons.

was done using both PSORT (plants) and PSORTII (animals). PSORTII predicted four potential nuclear localization signals, three (positions 31, 48, and 60) in the amino-terminal and one in the carboxy-terminus (245) of NumA1 (Fig. 3A) [1]. Further to this, a bulky phenylalanine residue at position 37 flanks the NLS predicted by PSORTII at position 31, which is uncommon for typical NLSs. In contrast, PSORT predicted only two of these (positions 48 and 60; Fig. 3A). Thus, both PSORT and PSORTII predict that the N-terminal portion of NumA1 contains two overlapping basic amino acid clusters (48–64 and 61–64; Fig. 1A). To test the ability of these domains and the CaMBD to direct NumA1 into the nucleus, a series of NumA1 deletion constructs fused to the C-terminus of GFP were generated (Fig. 1B).

Transfection of *Dictyostelium* with each fusion construct in all but one case generated a fusion protein of the expected molecular weight as detected by Western blotting using anti-GFP antibody (Fig. 3C). Control AX3 cells were negative for GFP. However, as detailed below, cells carrying pGFPNumAΔ48–64EF, although resistant to the antibiotic G418, did not express the fusion protein to any detectable level (Fig. 3C). The subcellular localization of each GFP-construct was analyzed by fluorescence microscopy. GFP alone was scattered uniformly throughout the cell with no evidence of nuclear localization (Fig. 4A, left panel). Cells transfected with full length GFP-NumA1 showed a distinct distribution at the internal periphery of nuclei which is in keeping with previous work (Fig. 4A, middle panel) [1]. As seen in these pictures and as detailed below, axenic strains of *Dictyostelium* cells grown in liquid culture contain mainly (~72%) uninucleate cells with a significant percentage (~23%) of binucleates and few multinucleate cells. Cells transformed with pGFP-NumAΔ118–167 not only demonstrated the peripheral intranuclear localization of NumA1 but also exhibited the highly multinucleate phenotype common to cells expressing NumA1 constructs lacking the DEED domain (Fig. 4A, right panel). Cells transformed with pGFPNumAΔC211 show a distinct nuclear localization

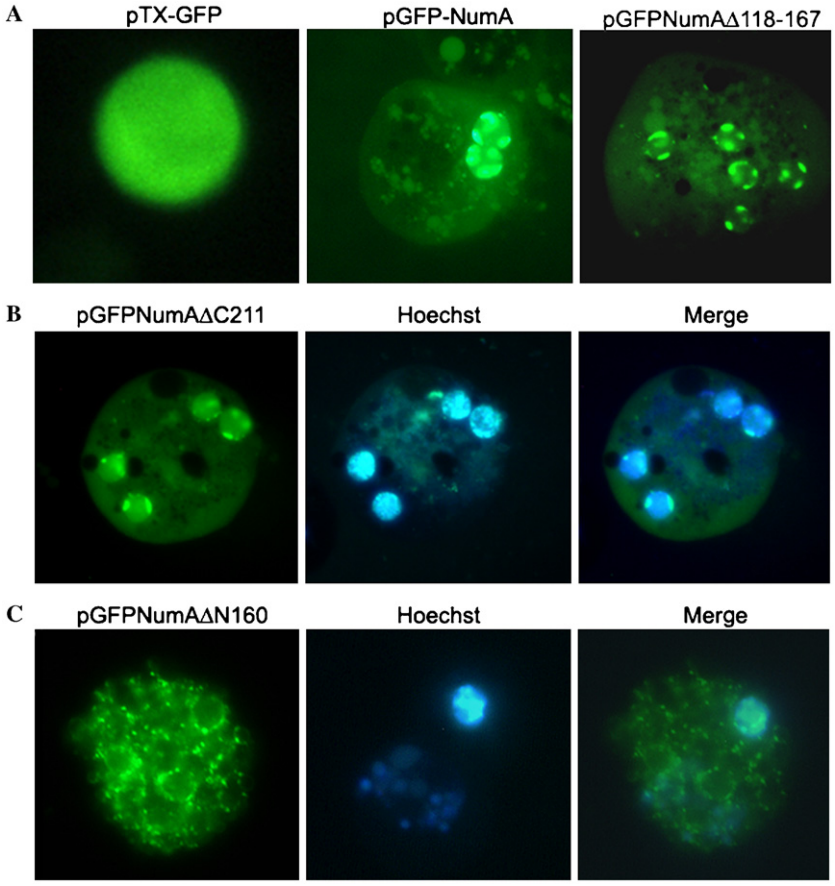

Fig. 4. Localization of GFP-NumA1 deletion constructs in vegetative cells. (A) Cultures of *D. discoideum* AX3 cells that were transfected with the GFP-NumA1 deletion constructs shown in Fig. 1 were analyzed for GFP localization by epifluorescence microscopy. Control cells transfected with pTX-GFP (left panel). Cells transfected with GFP-NumA1 (middle panel). Cells transfected with GFP-NumAΔ118–167 (right panel). (B) GFP-localization in cells transfected with GFPNumAΔC211 (left panel); nuclear staining with Hoechst 33258 (middle panel); computer-assisted image overlay (right panel). (C) GFP-fluorescence in cells transfected with GFPNumAΔN160 (left panel); Hoechst 33258 (middle panel); image overlay (right panel).

that appears identical to that seen in cells expressing either GFP-NumA1 or GFPNumAΔ118–167 (Figs. 2B and C). Computer-assisted overlay of pGFP-NumAΔC211 (Fig. 4B, left panel) and Hoechst (Fig. 4B, center panel) verified that GFP fluorescence for these constructs was localized within nuclei (Fig. 4B, right panel). This construct lacked the C-terminal sequence at position 245–252 that was identified by PSORTII as a potential NLS, thus revealing it is not involved in nuclear translocation. Also, since the pGFP-NumAΔC211 construct also lacks the identified CaMBD, this indicates that CaM-binding to NumA1 is not required for its movement into the nucleus or for its intranuclear localization.

The NumA1 bipartite NLS increases the distribution of GFP fluorescence in nuclei

When cells were transformed with pGFP-NumAΔN160 lacking the overlapping NLS detected by PSORT, they did not show any nuclear fluorescence within the nucleus (Fig. 2C). Instead punctate fluorescence was present throughout the cytoplasm (Fig. 2C, left panel). Hoechst staining of nuclei verified the non-nuclear distribution of pGFPNumAΔN160 (Fig. 2C, center and right panel). To test the ability of the N-terminal putative NLS residues ^{48}KKSYQDPEIIAHSRPRK^{64} to direct a protein into the nucleus, we generated a C-terminal fusion of this domain alone to GFP. The resulting construct was sequenced to verify that the fusion protein carried the desired in-frame addition. Cells transformed with pGFP-^{48}NLS^{64} were analyzed for cellular localization by fluorescence microscopy (Figs. 5A–D). Cells transfected with pGFP-^{48}NLS^{64} show an increased nuclear distribution of GFP fluorescence that is not seen in cells transfected with GFP alone. Cells stained with Hoechst verified the observed increased nuclear localization of pGFP-^{48}NLS^{64} and a computer-assisted overlay of pGFP-^{48}NLS^{64} and Hoechst clearly shows increased GFP fluorescence localized within Hoechst stained nuclei (Figs. 5A1–3). Individual cells transfected with pGFP-^{48}NLS^{64} revealed varying intensities of the nuclear localization (Figs. 5B–D). The lack of evidence of peripheral staining of these nuclei characteristic of full length and ΔDEED constructs suggests that additional amino-terminal attributes are required for the distribution of NumA1 to the internal periphery of nuclei. The fact that some of the cells transfected with pGFP-^{48}NLS^{64} showed a significant level of cytoplasmic fluorescence could be due to a number of factors. First it may be artifact in some cells, which show extremely large intranuclear accumulations with the resulting intense fluorescence of the pGFP-^{48}NLS^{64} seeming to extend into the cytoplasm (Fig. 5D). In other cases, premature proteolysis of the fusion protein could remove the NLS causing it to remain in the cytoplasm. However, this scenario does not seem likely, as Western blots do not show any detectable degradation products in cells expressing this GFP fusion protein. Kinases also affect nuclear import of some proteins through phosphorylation at or near site(s) close to the NLS. Phosphorylation of the NLS or critical residues in NumA1 that surround the predicted NLS could also be required for its maximal localization to nuclei. Phosphorylation sites for casein kinase II (CKII) and the cyclin-dependent kinase serve to regulate nuclear localization of the NLS-containing SV40 large T antigen, and that these modifications determine both the rate and amount of SV40 large T antigen that accumulates in the nucleus [25]. In keeping with this, NumA1 contains at least two predicted CKII phosphorylation sites. One site is found

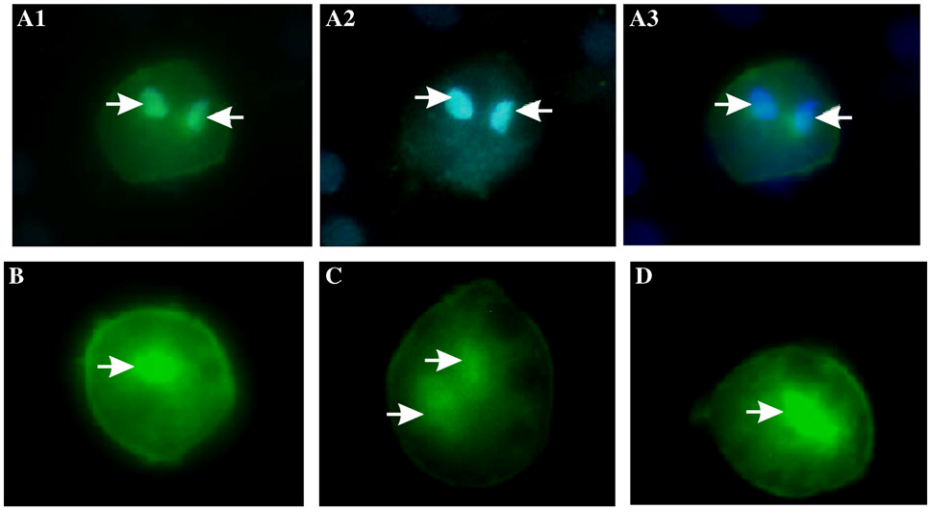

Fig. 5. The NumA1 nuclear localization signal increases GFP distribution in nuclei. (A1–3) GFP fluorescence in an individual cell transfected with GFP^{48}NLS^{64} (A1); Hoechst 33258 (A2); computer-assisted image overlay (A3). (B–D) Three individual cells transformed with GFP^{48}NLS^{64}. Arrows in the figure indicate nuclei.

at positions 50–53 within the amino-terminal bipartite NLS and another positioned at residues 70–73 downstream of the NLS. The significance of these sites to nuclear accumulation or import of NumA1 remains to be investigated.

Site-directed mutagenesis of the NumA1 bipartite NLS produces an unstable protein

The identification of the bipartite NLS does not rule out other means of regulating the nuclear import or export of NumA1. It is also possible that the sequence at position 31 by PSORTII may function in nuclear import. To further test if residues ^{48}KKSYQDPEIIA HSRPRK^{64} alone defined the subcellular localization of NumA1, GFP fusion constructs were generated in which the bipartite NLS was mutated to ^{48}EF^{49}. This approach has successfully been used to study the role of the NumA1 DEED domain in regulating nuclear number and in assessing its binding to calcium-binding protein 4a [1,26]. The resultant plasmid construct encoding the fusion protein GFPNumAΔ48–64EF was verified by sequencing and transformed into *Dictyostelium* strain AX3. Transformants were readily obtained that were resistant to the antibiotic G418 in 15 separate experiments. Cells transformed with GFPNumAΔ48–64EF appeared healthy morphologically and when stained with Hoechst showed the presence of nuclei (Fig. 6A, left panel). However, no GFP fluorescence could be detected in these cells (Fig. 6A, right panel). This absence of fluorescence was surprising since the compact protein structure of GFP alone makes it very stable under a number of physiological conditions including protease treatment [27]. Thus, one would expect to detect some level of GFP fluorescence even if the mutant fusion protein backbone was disrupted due to misfolding at the site of mutagenesis. Other studies have shown that the fusion of degradation domains to GFP can effectively destabilize GFP through the significant decrease in its cellular half-life [28]. Similarly, *Arabidopsis* protoplasts transformed with GFP show no detectable GFP fluorescence [29]. Unfortunately, previous studies had not elucidated the reasons why certain GFP-constructs do not result in observable fluorescence.

The inability to detect GFPNumAΔ48–64EF may be related to protein stability

Since this result could have impact on future studies, we analyzed four independent G418-resistant GFP-NumAΔ48–64EF transformants for the presence of endogenous NumA1 protein. As seen in Fig. 6B, endogenous NumA1 is readily detected in Western blots with anti-NumA1. When the same cells were analyzed for the presence of GFPNumAΔ48–64EF using anti-GFP, no signal was detected for GFPNumAΔ48–64EF or GFP

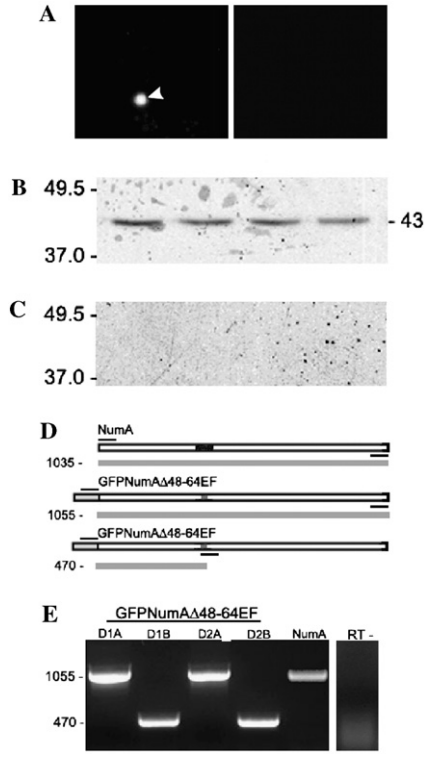

Fig. 6. Deletion of the amino-terminal bipartite NLS affects GFP-NumA1 stability. (A) Fluorescence of cell transformed with GFP-NumAΔ48–64EF: Hoechst 33258 (left panel); GFP (right panel). Western analysis of endogenous NumA1. Western blots of cells from four independent cultures were probed (B) with purified polyclonal anti-NumA1 antibodies; MW (kDa) of NumA1 is shown on the right) or (C) with monoclonal anti-GFP. (D) Schematic and predicted sizes of RT-PCR amplified NumA1 fragments. Primer pairs and their corresponding target sequences are shown (black lines) Expected PCR products are shown as gray bars with the expected sizes in base pairs shown on the left. (E) Expression of GFPNumA48–64EF and endogenous NumA1 mRNA. Total RNA was analyzed using RT-PCR from representative clones that were negative for the detection of both GFP fluorescence and fusion protein via Western analysis. RT-PCR was carried out using gene specific primers to GFP, NumA1, and the incorporated NLS deletion. D1A, GFPNumA48–64EF full-length transcript; D1B, GFPNumA48–64EF internal deletion transcript; D2A, GFPNumA48–64EF full-length transcript; D2B, GFP-NumA48–64EF internal deletion transcript; NumA1, endogenous NumA1; RT−, negative control. Molecular size markers for protein (kDa) and RNA (bp) are shown on the left.

alone (Fig. 6C). On the other hand using gene specific primers for GFP, NumA1 and the incorporated in-frame deletion of the amino-terminal NLS appropriate length mRNA transcripts were successfully amplified from transfected cells (Figs. 6D and E). This suggests that the mRNA produced in cells transfected with GFP-NumAΔ48–64EF is stable with destabilization occurring at the protein level. While the inability to express NumA1 protein containing the deleted identified NLS rules out its use for further intracellular localization studies, it was still possible to assess the impact of this construct on cell function. Since NumA is involved in

regulating nuclear number and, for a number of other reasons, implicated in cell cycle we analyzed the growth of cells expressing the various constructs [6].

Growth of cells expressing GFP-constructs

To see if cells transfected with the GFPNumAΔ48–64EF deletion mutant grew at the same rate as AX3 or other GFP-NumA1 deletion mutants, the average cell density was calculated and plotted logarithmically over time (Fig. 7). Interestingly, although all of the cells showed a normal morphology in liquid culture, those transfected with GFPNumAΔ48–64EF exhibited a markedly slower growth rate in liquid culture compared to wild type cells or those expressing other GFP-constructs. GFPNumAΔ48–64EF cells showed delayed growth for at least 2 days with ~90% inhibition evident after 4 days (Fig. 7). This suggests that even transient GFPNumAΔ48–64EF expression and failure to translocate to the nucleus can affect cell growth.

Nuclear localization of NumA1 is required for its function

As a nuclear CaMBP, NumA1 has been shown to be involved in regulating the number of nuclei per cell through some mechanism associated with its DEED domain [1]. Yeast two-hybrid and coimmunoprecipitation studies have revealed that the calcium-binding protein CBP4a binds to NumA1 via the DEED domain in a calcium-dependent manner but the role of this interaction remains unknown [26]. To learn more about the role of various regions of NumA1 in affecting nuclearity, the number of nuclei was counted for cells transfected

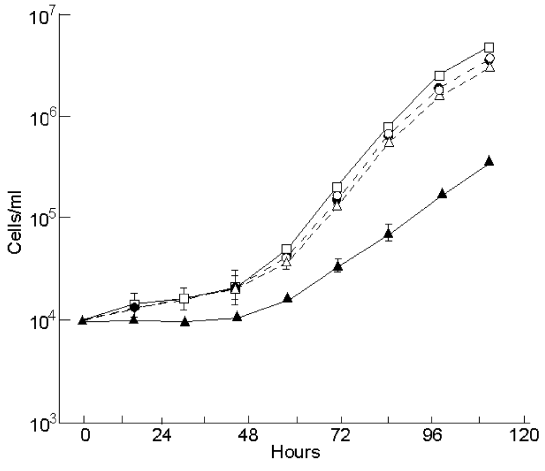

Fig. 7. Growth of *Dictyostelium* cells expressing various GFP-constructs. Growth curves of AX3 and AX3 cells transformed with GFP-NumA1 deletion constructs. Mean cell density (cells/mL) was calculated using a hemocytometer and plotted logarithmically over time (h). A sample size of $n = 16$ was used for each data point. Key: AX3 (-□-); GFP (-●-); GFPNumAΔC211 (-○-); GFPNumAΔN160 (-△-); GFPNumAΔ48–64EF (-▲-).

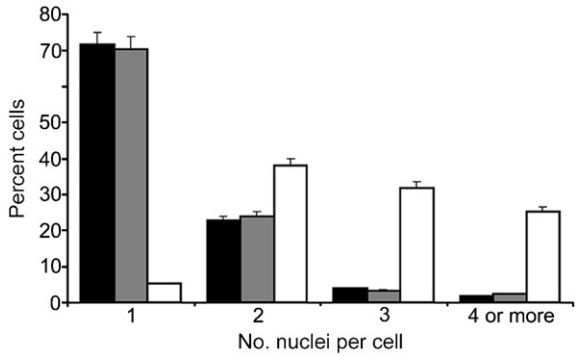

Fig. 8. Nuclear localization of GFPNumAΔC211 induces multinuclearity. Nuclei were counted from cells expressing GFP-NumA1 deletion constructs. Cell expressing GFPNumAΔC211 leads to an increase in multinuclear cells in shaking cultures. The nuclei of about 300 cells were counted for each transformant. Black bars, GFP-NumA1; gray bars, GFPNumAΔN160; white bars, GFPNumAΔC211. Values are means ± SEM for three experiments. $P < 0.005$.

with GFP-NumA1, pGFPNumAΔN160, and pGFP-NumAΔC211 (Fig. 8). In keeping with earlier work, the majority of the cells expressing GFP-NumA1 were uninucleate (71.5 ± 4%) while 22.7 ± 2.1% were binucleate with only ~2% possessing three or more nuclei [1]. In that work, a GFP-construct lacking the DEED domain, but possessing the NLS identified here, localized within nuclear patches producing populations in which over 90% of the cells possessed multiple nuclei. In support of those results, pGFPNumAΔC211, which lacks the DEED sequence but has the NLS, consistently displayed a significant increase in multinuclearity with ~95% of the cells possessing two or more nuclei and ~25.2 ± 3.5% with four or more nuclei (Fig. 8). However, cells expressing pGFPNumAΔN160, a construct lacking both the DEED domain and the NLS, appear like control cells with mainly uninucleate (~70.3 ± 6%) and binucleate (~24.4 ± 3.1%) cells and very few (~2.3%) multinucleates (Fig. 8). These results further support the role of the DEED domain in regulating nuclear number and they indicate that nuclear localization of NumA1 is required to carry out this function.

While the NLS determined here is sufficient to localize NumA1 to the nucleus, it does not reveal how NumA1 becomes localized as dense plaques at the internal periphery of *Dictyostelium* nuclei as seen in full length constructs. Previous work ruled out the transmembrane domain as functioning to subcompartmentalize NumA1 [1]. That conclusion is supported here with construct pGFPNumAΔC211, which lacked the Tm domain but still localizes as dense patches near the nuclear periphery. Similarly, the work presented here rules out calmodulin-binding as being essential to this process. In total, these results suggest that the certain as yet undetermined amino-terminal residues somehow mediate the localization of GFP-NumA1 to the nuclear periphery.

Acknowledgment

A grant from the Natural Sciences and Engineering Research Council of Canada supported this work.

References

[1] M.A. Myre, D.H. O'Day, Nucleomorphin: a novel, acidic, nuclear calmodulin-binding protein from *Dictyostelium* that regulates nuclear number, J. Biol. Chem. 277 (2002) 19735–19744.
[2] M.A. Myre, D.H. O'Day, *Dictyostelium* nucleomorphin is a member of the BRCT-domain family of cell cycle checkpoint proteins, Biochem. Biophys. Acta, Gen. Subj. 1675 (2004) 192–197.
[3] E.E. Capowski, J.W. Tracy, Ribosomal RNA processing and the role of SmMAK16 in ribosome biogenesis in *Schistosoma mansoni*, Mol. Biochem. Parasitol. 132 (2003) 67–74.
[4] A. Marchler-Bauer, J.B. Anderson, C. DeWeese-Scott, N.D. Fedorova, L.Y. Geer, S. He, D.I. Hurwitz, J.D. Jackson, A.R. Jacobs, C.J. Lanczycki, C.A. Liebert, C. Liu, T. Madej, G.H. Marchler, R. Mazumder, A.N. Nikolskaya, A.R. Panchenko, B.S. Rao, B.A. Shoemaker, V. Simonyan, J.S. Song, R.A. Thiessen, S. Vasudevan, Y. Wang, R.A. Yamashita, J.J. Yin, S.H. Bryant, CDD: a curated Entrez database of conserved domain alignments, Nucleic Acids Res. 31 (2003) 383–387.
[5] R.B. Wickner,, Host function of MAK16: G1 arrest by a mak16 mutant of *Saccharomyces cerevisiae*, Proc. Natl. Acad. Sci. USA 85 (1988) 6007–6011.
[6] M.A. Myre, Characterization of nucleomorphin, a novel nuclear breast cancer carboxy-terminal-domain containing calmodulin-binding protein from *Dictyostelium discoideum*, PhD Thesis, University of Toronto (2005).
[7] D. Gorlich, U. Kutay, Transport between the cell nucleus and the cytoplasm, Annu. Rev. Cell Dev. Biol. 15 (1999) 607–660.
[8] J. Robbins, S.M. Dilworth, R.A. Laskey, C. Dingwall, Two interdependent basic domains in nucleoplasmin nuclear targeting sequence: identification of a class of bipartite nuclear targeting sequence, Cell 64 (1991) 615–623.
[9] T.D. Sweitzer, J.A. Hanover, Calmodulin activates nuclear protein import: a link between signal transduction and nuclear transport, Proc. Natl. Acad. Sci. USA 93 (1996) 14574–14579.
[10] A. Argentaro, H. Sim, S. Kelly, S. Preiss, A. Clayton, D.A. Jans, V.R. Harleya, A SOX9 defect of calmodulin-dependent nuclear import in campomelic dysplasia/autosomal sex reversal, J. Biol. Chem. 278 (2003) 33839–33847.
[11] Å. Antonsson, K. Hughes, S. Edin, T. Grundström, Regulation of c-Rel nuclear localization by binding of Ca^{2+}/calmodulin, Mol. Cell. Biol. (2003) 1418–1427.
[12] S.M. Lemrow, K.A. Anderson, J.D. Joseph, T.J. Ribar, P.K. Noeldner, A.R. Means, Catalytic activity is required for calcium/calmodulin-dependent protein kinase IV to enter the nucleus, J. Biol. Chem. 279 (2004) 11664–11671.
[13] A.M. Moerman, C. Klein, *Dictyostelium discoideum* Hsp32 is a resident nucleolar heat-shock protein, Chromosoma 107 (1998) 145–154.
[14] H. Van Der Wel, H.R. Morris, M. Panico, T. Paxton, A. Dell, L. Kaplan, C.M. West, Molecular cloning and expression of a UDP-*N*-acetylglucosamine (GlcNAc):hydroxyproline polypeptide GlcNAc-transferase that modifies Skp1 in the cytoplasm of *Dictyostelium*, J. Biol. Chem. 277 (2002) 46328–46337.
[15] N.V. Zhukovskaya, M. Fukuzawa, M. Tsujioka, K.A. Jermyn, T. Kawata, T. Abe, M. Zvelebil, J.G. Williams, Dd-STATb, a *Dictyostelium* STAT protein with a highly aberrant SH2 domain, functions as a regulator of gene expression during growth and early development, Development 131 (2003) 447–458.
[16] D. Kalderon, B.L. Roberts, W.D. Richardson, A.E. Smith, A short amino acid sequence able to specify nuclear location, Cell 39 (1984) 499–509.
[17] A. Persechini, R.H. Kretsinger, The central helix of calmodulin functions as a flexible tether, J. Biol. Chem. 263 (1988) 12175–12178.
[18] K.T. O'Neil, W.F. DeGrado, Calmodulin signaling via the IQ motif, Trends Biol. Sci. 15 (1990) 59–64.
[19] K.L. Yap, J. Kim, K. Truong, M. Sherman, T. Yuan, M. Ikura, Calmodulin target database, J. Struct. Funct. Genomics 1 (2000) 8–14.
[20] M. Bahler, A. Rhoads, Calmodulin signalling via the IQ-motif, FEBS Lett. 513 (2002) 107–113.
[21] J.D. Moore, J. Yang, R. Truant, S. Kornbluth, Nuclear import of cdk/cyclin complexes: identification of distinct mechanisms for import of cdk2/cyclin E and cdc2/cyclin B1, J. Cell Biol. 144 (1999) 213–224.
[22] L. Hauser, M. Dhar, D. Olins, *Dictyostelium discoideum* contains a single-copy gene encoding a unique subtype of histone H1, Gene 154 (1995) 119–122.
[23] M.A. Myre, D.H. O'Day, Calmodulin binds to and inhibits the activity of phosphoglycerate kinase, Biochim. Biophys. Acta, Mol. Cell Res. 1693 (2004) 177–183.
[24] D.H. O'Day, Calmodulin-mediated signaling in *Dictyostelium discoideum*: CaMBOT isolation and characterization of the novel poly-domain protein nucleomorphin and other calmodulin-binding proteins, in: F. Columbus (Ed.), Progress in Cellular Signalling Research, Nova Publications, New York, 2005.
[25] D.A. Jans, The regulation of protein transport to the nucleus by phosphorylation, Biochem. J. 311 (1995) 705–716.
[26] M.A. Myre, D.H. O'Day, *Dictyostelium* calcium-binding protein 4a interacts with NumA, a BRCT-domain protein that regulates nuclear number, Biochem. Biophys. Res. Commun. 322 (2004) 655–671.
[27] M. Chalfie, G. Euskirchen, W.W. Ward, D.C. Prasher, Green fluorescent protein as a marker for gene expression, Science 263 (1994) 802–805.
[28] X. Li, X. Zhao, Y. Fang, X. Jiang, T. Duong, C. Fan, C.C. Huang, S.R. Kain, Generation of destabilized green fluorescent protein as a transcription reporter, J. Biol. Chem. 273 (1998) 34970–34975.
[29] W. Hu, C.L. Cheng, Expression of *Aequorea* green fluorescent protein in plant cells, FEBS Lett. 369 (1995) 331–334.
[30] S.W. Vetter, E. LeClerc, Novel aspects of calmodulin target recognition and activation, Eur. J. Biochem. 270 (2003) 404–414.